

## Lehigh University Lehigh Preserve

---

### Theses and Dissertations

---

1-1-1981

# Sipos resistors doped by ion implantation.

Richard James Snyder

Follow this and additional works at: <http://preserve.lehigh.edu/etd>



Part of the [Electrical and Computer Engineering Commons](#)

---

### Recommended Citation

Snyder, Richard James, "Sipos resistors doped by ion implantation." (1981). *Theses and Dissertations*. Paper 1997.

This Thesis is brought to you for free and open access by Lehigh Preserve. It has been accepted for inclusion in Theses and Dissertations by an authorized administrator of Lehigh Preserve. For more information, please contact [preserve@lehigh.edu](mailto:preserve@lehigh.edu).

**SIPOS RESISTORS DOPED  
BY ION IMPLANTATION**

**by  
Richard James Snyder**

**A Thesis**

**Presented to the Graduate Committee  
of Lehigh University  
in Candidacy for the Degree of**

**Master of Science  
in  
Electrical Engineering**

**Lehigh University**

**1981**

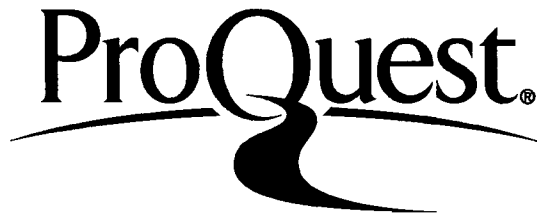
ProQuest Number: EP76270

All rights reserved

INFORMATION TO ALL USERS

The quality of this reproduction is dependent upon the quality of the copy submitted.

In the unlikely event that the author did not send a complete manuscript and there are missing pages, these will be noted. Also, if material had to be removed, a note will indicate the deletion.



ProQuest EP76270

Published by ProQuest LLC (2015). Copyright of the Dissertation is held by the Author.

All rights reserved.

This work is protected against unauthorized copying under Title 17, United States Code  
Microform Edition © ProQuest LLC.

ProQuest LLC.  
789 East Eisenhower Parkway  
P.O. Box 1346  
Ann Arbor, MI 48106 - 1346

This thesis is accepted and approved in partial fulfillment of the requirements for the degree of Master of Science in Electrical Engineering.

Oct. 23, 1981

(date)

Professor in Charge

Chairman of Department

## ACKNOWLEDGEMENTS

The author wishes to express his thanks to his supervisor, J. R. Mathews, for supplying the information which led to the selection of the topic. Also he wishes to thank his department head, R. L. Batdorf, and supervisor for critically reading and supporting the work. Finally he wishes to thank his thesis advisor, F. Hielscher for advice and suggestions on the topic and for critically reading the manuscript.

## TABLE OF CONTENTS

	<u>Page No.</u>
I. <u>INTRODUCTION</u>	3
II. <u>SIPOS RESISTOR USEFULNESS</u>	8
A. DOPED SIPOS OFFERS $50\text{K}\Omega/\square$ SHEET RESISTANCE	
B. DOPED SIPOS RESISTOR PROCESS DESIGN OFFERS ADDITIONAL BENEFITS	
III. <u>RESISTOR PROCESSING</u>	12
A. SIPOS PROCESS	
B. PLASMA ETCHING OF SIPOS RESISTOR	
IV. <u>SHEET RESISTANCE OF IMPLANT DOPED SIPOS</u>	17
A. DOPANT AND DOSE EFFECTS ON RESISTIVITY	
B. FOUR POINT PROBE VERSUS ACTUAL RESISTOR SHEET RESISTANCE	
C. SENSITIVITY OF RESISTIVITY ON ION IMPLANT DOSE	
D. RESISTIVITY VARIATION DUE TO ATOMIC PERCENT OF OXYGEN	
V. <u>RESISTOR PROPERTIES</u>	24
A. CONTACT RESISTANCE OF SIPOS RESISTORS	
B. TEMPERATURE COEFFICIENT OF RESISTANCE	
C. LINEARITY OF SIPOS RESISTORS	

	<u>Page No.</u>
VI. <u>ELEMENTARY PHYSICS OF IMPLANTED SIPOS RESISTOR STRUCTURES</u>	28
A. HIGH CONCENTRATION REGION	
B. LOW CONCENTRATION REGION	
C. POLYSILICON AND SIPOS SIMILARITIES AND DISSIMILARITIES	
VII. <u>RESISTOR TEST PATTERN</u>	37
A. TEST PATTERN ELEMENTS	
B. TEST PATTERN RESULTS	
VIII. <u>CONCLUSIONS</u>	48

IX. LIST OF TABLES

Page No.

TABLE NUMBER

TITLE

1	RESISTOR PROCESS	13
2	SHEET RESISTANCE	19

X. LIST OF FIGURES

FIGURE NUMBER

TITLE

1	SIPOS RESISTOR STRUCTURE	6
2	ACTIVE FILTERS	11
3	IMPLANTED SIPOS RESISTOR PROCESS	14
4	SHEET RESISTANCE VS. IMPLANT DOSE	18
5	RESISTANCE OF SIPOS FILM	20
6	SENSITIVITY OF SIPOS RESISTIVITY TO VARIOUS PROBE PRESSURES	26
7	CURRENT VOLTAGE SLOPE DEPENDENCE ON IMPLANT DOSE	29
8	LINEARITY OF A BORON DOPED 19% OXYGEN CONCENTRATION SIPOS RESISTOR	30
9	RESISTANCE OF IMPLANTED POLYSILICON	33
10	POLYSILICON RESISTORS HAVING SHORT LENGTHS	34
11	VARIOUS RESISTOR LENGTHS	35
12	ELEMENTS OF TEST PATTERN	38
13	SIPOS RESISTORS - RESISTOR END CONTACT TEST	39



<u>FIGURE NUMBER</u>	<u>TITLE</u>	<u>Page No.</u>
14	SIPOS RESISTORS - RESISTOR LENGTH TEST	40
15	SIPOS RESISTORS - RESISTOR WIDTH TEST	41
16	SIPOS RESISTORS - RESISTOR MEANDER TEST	42
17	LAYOUT OF TEST CHIP	43
18	WIDENING EFFECT OF RESISTOR BODY NEAR CONTACT END	46
19	ROUNDING EFFECT OF RESISTOR MEANDER	47
XI.	BIOGRAPHY	54

# ABSTRACT

SIPOS (Semi-Insulating Polycrystalline Oxygen Doped Silicon) is a semi-insulating material with resistivity in the range of  $10^6$ - $10^{14}$   $\Omega$ -cm at room temperature. SIPOS films have been generally used to provide high voltage discrete and integrated devices. By heavily doping the film with phosphorus during chemical vapor deposition, these films can be made moderately conductive. Vertical ballast resistors have been fabricated successfully with this technique and material. The motivation of the present investigation is to study SIPOS films doped by ion implantation, and to assess their potential to provide high value per square resistors adaptable to bipolar linear integrated circuits.

Linear circuit applications occasionally require resistance in the  $1M\Omega$  to  $50M\Omega$  range. Since standard diffused resistors typically don't exceed  $1000$ - $2000$   $\Omega/\square$ , resistors of this magnitude would require an exorbitant amount of silicon chip area. This need for high sheet resistance prompted an investigation of doped SIPOS to supply sheet resistance in the  $5K\Omega/\square$  to  $500K\Omega/\square$  range. The combination of LPCVD (Low Pressure Chemical Vapor Deposition) film deposition and ion implantation of the resulting film was undertaken to see if doped SIPOS would provide an easily manufacturable material with sufficient control to routinely produce films in the above sheet resistance range.

A modification of a linear integrated circuit process has been designed and fabricated to provide an oxide isolated nondiffused resistor having high sheet resistance. The modified process utilizes boron or phosphorus doped SIPOS to provide sheet resistance in the  $3.6\text{K}\Omega/\square$  to  $360\text{K}\Omega/\square$  range. The process provides resistors which are linear to  $2\text{KV}/\text{cm}$ . Between  $2\text{KV}/\text{cm}$  and  $6\text{KV}/\text{cm}$ , the resistance decreases by approximately 10%.

As measured by the four-point probe technique, sheet resistance of the impurity doped SIPOS films exhibited a critical sensitivity to ion implant dose similar to polysilicon. Actual resistance of the fabricated resistor differed somewhat from the four-point probe value for boron or phosphorus doped films. The difference in resistance is caused by the subsequent heat treatment and processing which are dissimilar for the four-point probe film and the completed resistor structure. SIPOS resistivity was found to be probe pressure sensitive. At the pressures typically used for four-point probe measurements, the sheet resistance was not affected. For 30KeV ion implant doses of  $10^{14}/\text{cm}^2$  and less, the SIPOS structure did not show a linear behavior. Instead the structure exhibited a bimodal conduction resembling a diode under reverse bias.

## I. INTRODUCTION

SIPOS is a semi-insulating polycrystalline silicon material doped with oxygen having a resistivity in the range of  $10^6$ - $10^{14}$   $\Omega$ -cm at room temperature. Aoki<sup>1</sup> et al studied the dependence of electrical resistivity of oxygen-doped films versus oxygen concentration and found that SIPOS resistivity increases as the atomic % of oxygen increases. SIPOS films have been used as high voltage insulators on discrete and integrated devices. Matsushita<sup>2</sup> et al used the SIPOS film and field-limiting rings as a replacement for the oxide passivation layer on planar devices to achieve npn and pnp transistors rated at 800V and 2500V. Mochizuki<sup>3</sup> et al utilized SIPOS on CMOS integrated circuit and did not need a channel-stopper diffusion required for the conventional oxide version, thus allowing higher packing density.

By doping the SIPOS film with phosphorus, Yamoto<sup>4</sup> et al fabricated vertical ballast resistors on transistors. The primary intent of this investigation is to study SIPOS resistors doped by ion-implantation and assess their potential for supplying high value per square resistors adaptable to integrated circuits. For bipolar linear integrated circuits, horizontal rather than vertical resistor structures are more desirable since one can design a wider range of resistance values with the horizontal structure.

Presently, bipolar linear integrated circuits utilize diffused and epitaxial regions of the process to provide resistors. Without adding any further processing steps, emitter, base, collector and pinch resistors are provided by the process and typically provide  $5 \Omega/\square$ ,  $200 \Omega/\square$ ,  $1250 \Omega/\square$  and  $10K \Omega/\square$ .<sup>5,6</sup> Frequently it is desirable to have resistances which are larger than the  $10K \Omega/\square$  value supplied by the pinch resistor but not subject to the disadvantages of the current technology. Pinch resistors are very nonlinear, exhibit high leakage current and have a high temperature coefficient of resistance. Thus, a modified bipolar linear integrated circuit process was designed to investigate the potential of doped SIPOS to supply five times the sheet resistance of pinch resistors ( $50K \Omega/\square$ ).

Since circuit applications occasionally demand resistance of  $1M\Omega$  to  $50M\Omega$ ,<sup>7,8</sup> a range of sheet resistance films around the  $50K\Omega/\square$  neighborhood was evaluated. The sheet resistance of SIPOS films was measured by the 4-point probe technique, and the resistance was characterized as a function of oxygen content and ion implant dose with a constant anneal condition of 1 hour at  $900^\circ\text{C}$ .

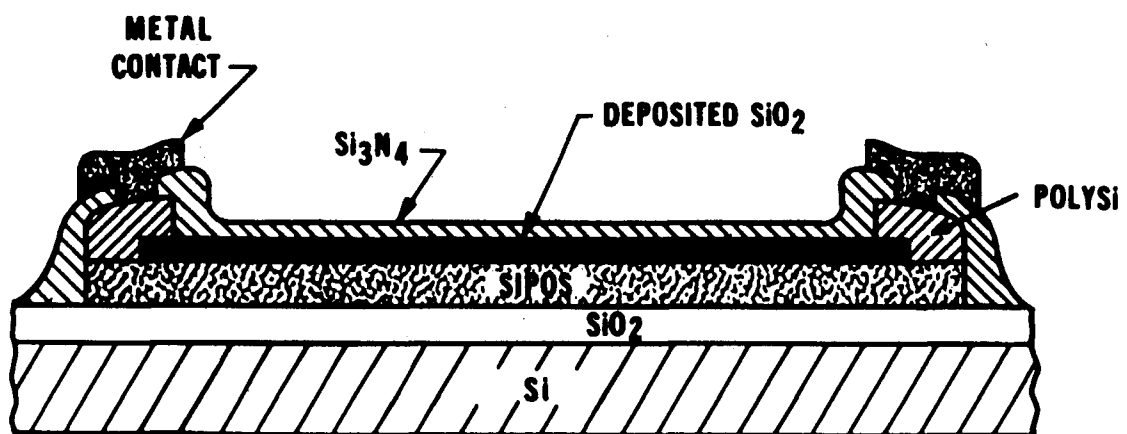
Ion implant doped SIPOS films were processed up to the polysilicon contact step at which time one can measure the sheet resistance of the film. Hence the films were characterized in terms of sheet resistance before any resistors were made.

Resistor test patterns were designed to study geometric effects on the resistance value as a function of the contact width, resistor

length, resistor width and resistor meander width. Next, a photolithographic mask set was fabricated to evaluate the resistor geometric effects and to determine various resistor characteristics. In particular, resistor reproducibility, contact resistance, linearity and temperature coefficient of resistance were measured.

Current integrated circuit processing technology utilizes plasma and chemical etching for pattern definition and both techniques were used in this study. In order to define the deposited oxide, the process employs a photoresist mask and chemical etching. The process employs both plasma etching with a photoresist mask and plasma etching with a deposited oxide mask to define the polysilicon contacts and the SIPOS resistor body, respectively. The process offers nondiffused crossovers which are available since polysilicon and a deposited oxide are added to the integrated circuit process.

Resistor structures were successfully fabricated and metalized as shown in Figure 1 with silicon nitride covering the resistor sidewall, thus sealing the resistor body. Two lots were processed and provided resistors in the  $50\text{K}\Omega/\square$  neighborhood. Contact resistance was found to be typically less than one square of sheet resistance and the temperature coefficient of resistance less than values obtained on pinch resistors. For low impurity doses, the SIPOS resistors exhibit a breakdown voltage, whereas at higher doses the resistors exhibit a nearly linear behavior. SIPOS and polysilicon similarities and dissimilarities are finally discussed.



**SIPOS RESISTOR STRUCTURE**

**FIGURE 1**

In essence a resistor replacement for pinch resistors and other high resistance applications has been designed, fabricated and electrically evaluated. The SIPOS resistor adds processing steps, but supplies numerous advantages. SIPOS resistor usefulness, resistor processing and sheet resistance of implant doped SIPOS are discussed in the first three sections. Resistor properties: contact resistance, temperature coefficient of resistance and resistor linearity are discussed in Section 5. Finally, a discussion of the elementary physics of implanted SIPOS resistor structures and the layout of the resistor test pattern are both described in the last sections.



## II. SIPOS RESISTOR USEFULNESS

Bipolar linear integrated circuits utilize the diffused and epitaxial regions of a wafer to provide resistors and crossunders. This is quite convenient since the emitter, base, collector and base under emitter regions of a wafer have typical sheet resistances of  $5 \Omega/\square$ ,  $200 \Omega/\square$ ,  $1250 \Omega/\square$  and  $10K \Omega/\square$ .<sup>5,6</sup> Thus the emitter diffusion provides a low resistance crossunder and the base, collector and base under emitter diffused/epitaxial regions provide a range of resistance for resistors.

Occasionally circuit applications require  $1M\Omega$  to  $50M\Omega$  resistors which for a collector sheet resistance of  $1250\Omega/\square$  would require an exorbitant amount of silicon chip area ( $12 \times 10^3 \mu m$  to  $6 \times 10^5 \mu m$  length for a  $15 \mu m$  wide resistor). For some applications, it is also desirable to have a high voltage per unit length of resistance. Pinch resistors provide  $10K \Omega/\square$  resistance; however, they are extremely nonlinear and in the case of the base under emitter pinch resistor will sustain only about six volts. A bulk pinch resistor will sustain up to nearly the collector base breakdown voltage but is also very nonlinear. Two other disadvantages of pinch resistors are that they have high temperature coefficients of resistance and that one cannot simply achieve voltage ratios by tapping off the geometric length of the resistor. The doped SIPOS resistor overcomes many of

these disadvantages and provides both high sheet resistance and crossovers for linear integrated circuits.

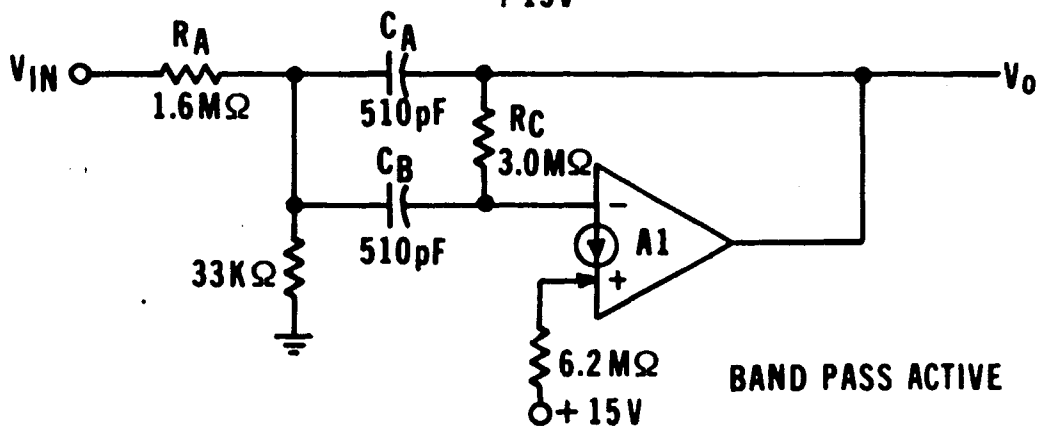
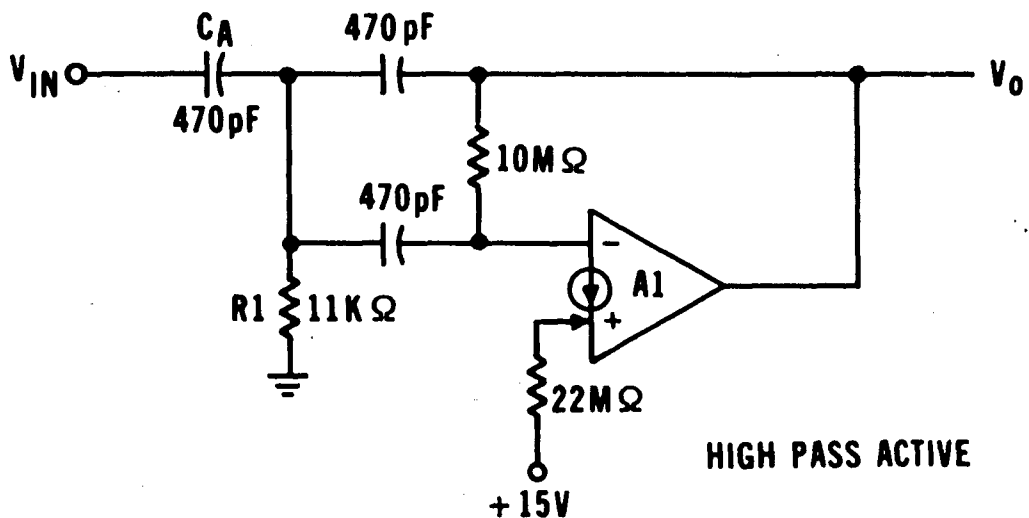
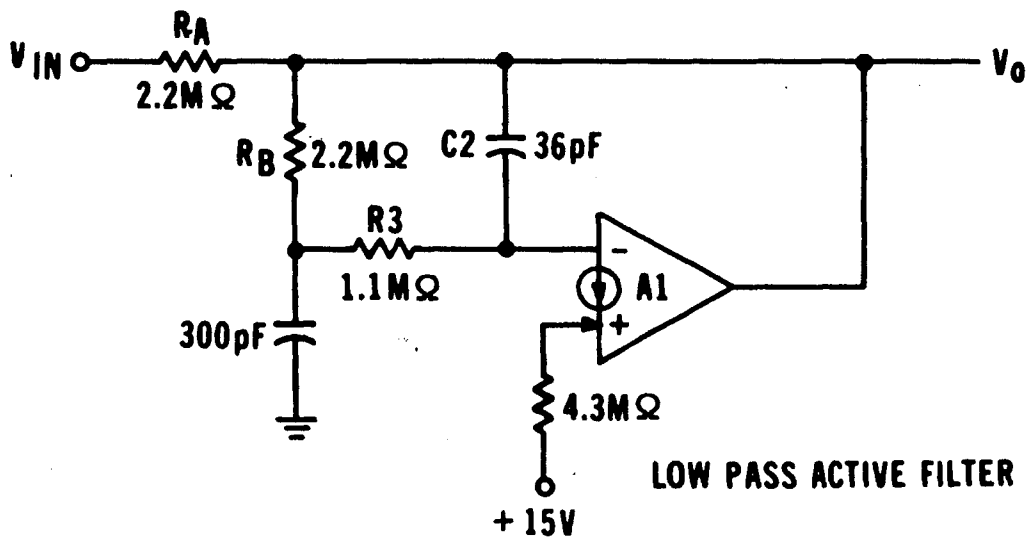
A. DOPED SIPOS OFFERS  $50\text{K}\Omega/\square$  SHEET RESISTANCE

A need exists for improved high value per square resistors on integrated circuits and recent work by Yamoto<sup>4</sup> et al indicates that phosphorus doped SIPOS offers this resistance, namely,  $50\text{K}\Omega/\square$ . Yamoto's method of doping the SIPOS was to dope it during deposition. In this investigation, the dopant, phosphorus or boron, was introduced into the material by ion implantation. Ion implantation was selected since controlled depths and doses can be achieved in SIPOS. SIPOS thickness variations would not affect the depth of the conducting portion of the film (only the annealing would affect the depth for a given film), thus minimizing a critical variable. A second reason for selecting ion implantation is that it provides more uniform distribution of the dopant in both the grain and grain boundary area of a film than would be provided by diffusion.

B. DOPED SIPOS RESISTOR PROCESS DESIGN OFFERS ADDITIONAL BENEFITS

The structural design of the doped SIPOS resistor provides numerous benefits. Comparing the doped SIPOS resistor to the diffused resistor, the SIPOS resistors have no junction leakage as is experienced by the standard diffused resistors; diffused resistors experience the saturation current of the reverse biased p-n junction surrounding the resistor. Another benefit provided by implant doped SIPOS is resistors capable of sustaining high voltages as well as

high voltages per unit length. The SIPOS resistors can sustain electric fields of 7KV/cm and higher before burning out. The resistors are linear up to electric fields of 2KV/cm and nearly linear up to 6KV/cm. Preliminary results indicate that the temperature coefficient of resistance is much better than that of pinch resistors and is in the neighborhood of the value of the diffused resistors. SIPOS resistors might be useful in low pass, high pass and bandpass active filters in a hybrid integrated circuit as shown in Figure 2<sup>7</sup> where the large capacitors would be supplied by using a very high quality (low defect density) deposited oxide. However, a 5000Å layer of SiO<sub>2</sub> would require approximately a 1500µm by 1500µm square area to produce a 470 pF capacitor, requiring a large amount of silicon chip area. SIPOS resistors may also help provide distributed RC networks for electrical filtering. Some electrical filters were designed in the test pattern; however, they were not processed due to a time limitation. Lastly, the polysilicon contact which is highly doped provides resistive crossovers; hence, both high resistance per square and crossunder limitations of linear integrated circuit processes are overcome.



**ACTIVE FILTERS**  
**FIGURE 2**

### III. RESISTOR PROCESSING

The steps of the high value per square resistor process are listed in Table 1 and result in the structure shown in Figure 1. The process is pictorially outlined in Figure 3 and sandwiched between the emitter and contact window steps of an integrated circuit process. It requires two additional photoresist steps to an integrated circuit process, one to define a deposited oxide over the resistor body and the second to define a polysilicon contact pad to the SIPOS resistor itself.

#### A. SIPOS PROCESS

Prior to the SIPOS resistive film deposition, a 1050°C thermal oxide was grown of 6000Å thickness. Next 2300Å-4550Å of 644°C SIPOS was deposited in a Low Pressure Chemical Vapor Deposition (LPCVD) system which uses nitrous oxide ( $N_2O$ ), silane ( $SiH_4$ ) and nitrogen ( $N_2$ ) gases. The oxygen content of the SIPOS film is controlled by adjusting the flow rate ratio of  $N_2O$  to  $SiH_4$ .<sup>1</sup> Many details of the deposition system and characteristics of the film have been described by Knolle and Maxwell.<sup>17,18</sup> Following the deposition, the SIPOS film was impurity doped at an energy of 30keV with boron or phosphorus. This energy was selected to allow for the projected depth range plus three standard deviations for the case of boron into amorphous  $SiO_2$ . Boron has a deeper depth range than phosphorus due to its small size and that depth is approximately 1900Å.<sup>8</sup> Next a 5000Å layer of silicon dioxide was deposited over the SIPOS at 892°C. Both films

TABLE 1

RESISTOR PROCESS

PHOTORESIST  
MASK LEVEL

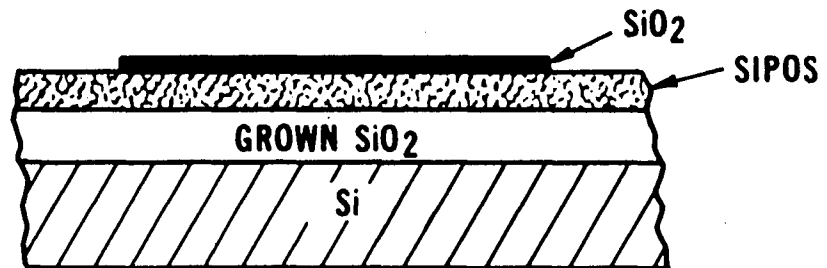
PROCESS

- |                   |   |
|-------------------|---|
|                   | 1. Grow 6000Å of SiO <sub>2</sub> at 1050°C                               |
|                   | 2. Deposit 3000Å of SIPOS (644°C)   |
|                   | 3. Ion Implant SIPOS (30 keV)   |
|                   | 4. Deposit 5000Å of SiO <sub>2</sub> (892°C)                              |
| SIPOS Level ----- | 5. Photoresist SiO <sub>2</sub> and Chemically Etch Off Excess            |
|                   | 6. Deposit 3000Å of Polysilicon (644°C)                                   |
|                   | 7. Ion Implant Polysilicon (30 keV) with $1.5 \times 10^{16}/\text{cm}^2$ |
| Poly Level -----  | 8. Photoresist Polysilicon  |
|                   | 9. Plasma Etch Off Excess Polysilicon and SIPOS                           |
|                   | 10. Subsequent Linear Integrated Circuit Processes                        |

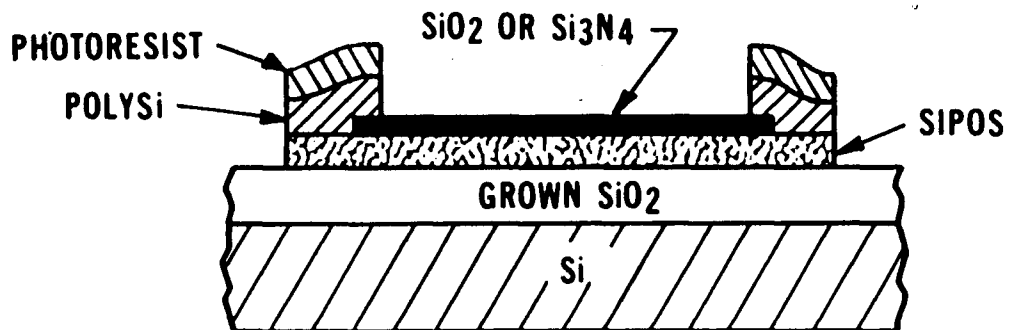
1. GROW  $\text{SiO}_2$ , DEPOSIT SIPOS, (IMPLANT), DEPOSIT  $\text{SiO}_2$



2. PHOTORESIST AND ETCH  $\text{SiO}_2$



3. DEPOSIT POLYSi, (IMPLANT), PHOTORESIST AND ETCH POLYSi AND ETCH SIPOS



4. STRIP RESIST

5. DEPOSIT NITRIDE

**IMPLANTED SIPOS RESISTOR PROCESS**

**FIGURE 3**

were deposited in a LPCVD system since this system offers better uniformity than the atmospheric CVD system. Note that the SIPOS film was partially annealed by the deposited oxide deposition process at this time.

At this point the oxide was covered with photoresist and etched. Unlike  $\text{SiO}_2$  and  $\text{Si}_3\text{N}_4$ , SIPOS is virtually insoluble in buffered HF. This allows one to deposit an oxide over the top of the SIPOS and then to photolithographically pattern and etch the oxide without significantly affecting the SIPOS layer underneath.

After the deposited oxide is patterned and etched, 3000<sup>o</sup>Å of polysilicon is deposited over the entire wafer and implanted at an energy of 30 keV and a dose of  $1.5 \times 10^{16}/\text{cm}^2$ . This film is next patterned into resistor contacts. A more desirable method of contacting the resistor is to dope the polysilicon in-situ. This would have eliminated the implant step and minimized contact resistance; however, doped polysilicon was unavailable at the time of the experiment. In the last part of the resistor process, the polysilicon is photoresisted and etched in a plasma reactor to remove the excess polysilicon and the excess SIPOS.

#### B. PLASMA ETCHING OF SIPOS RESISTOR

An IPC 2000 plasma reactor was used to etch the excess polysilicon and excess SIPOS. Initially, wafers were etched one at a time until the 1050°C thermal oxide color showed uniformly across the



wafer. This can be viewed through the see-through door of the plasma chamber.

The 1050°C thermal oxide was steam grown and has a much lower etch rate in the plasma than the deposited SIPOS or deposited oxide. Etch rates of the field oxide have been estimated to be one-tenth the rate of SIPOS in carbon tetrafluoride 14+4% oxygen gas. Prior to plasma etching, the slices were preheated to 100°C. Preheating speeds up the reaction, giving reasonable etch rates.

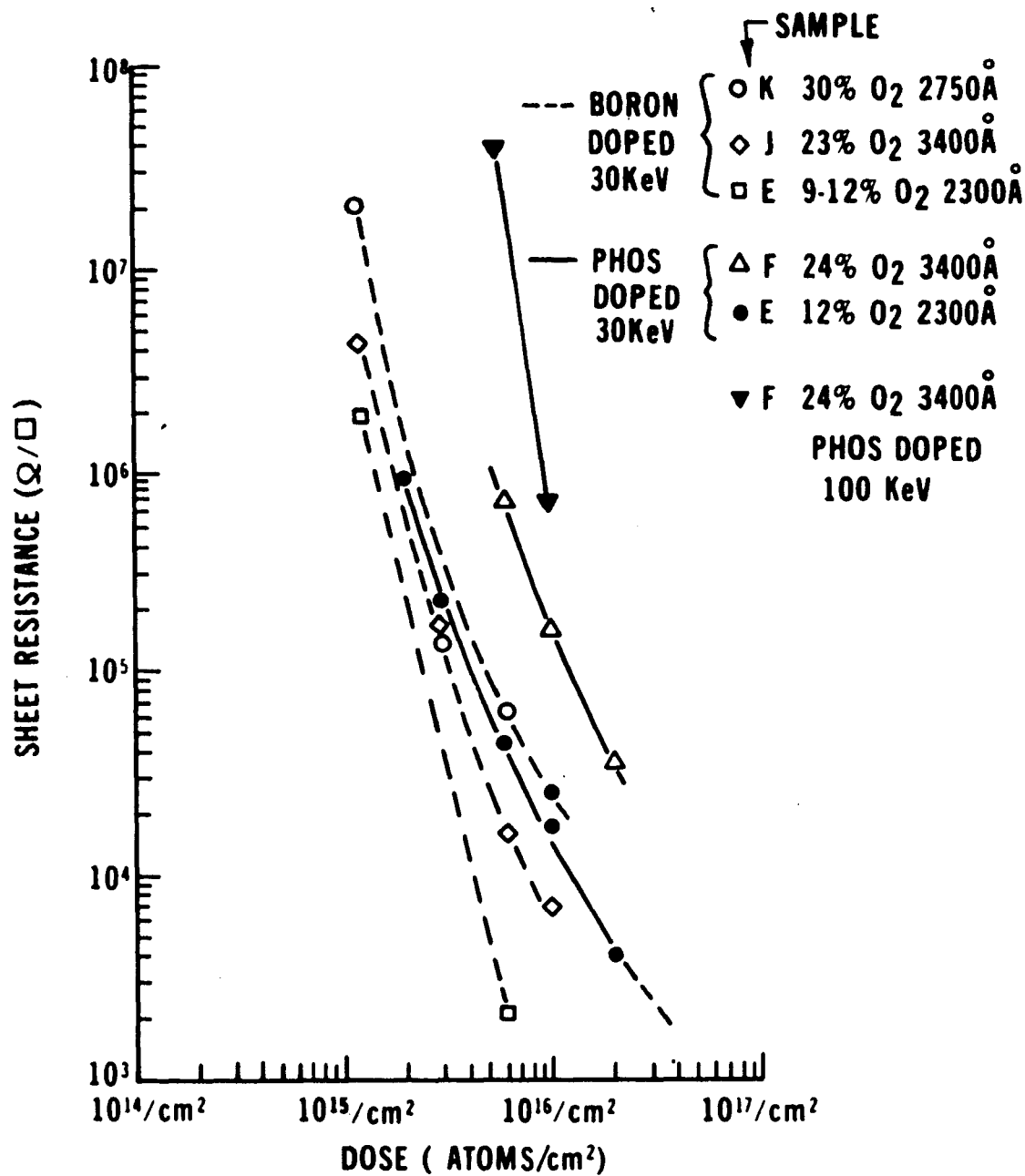
When wafers were etched one at a time, an etch rate of approximately 460Å/min. was obtained. If wafers were etched in quantities of approximately 10, the etch rate dropped to about 150Å/min. The leading wafers always etched more quickly, requiring sequential removal from the chamber; otherwise, severe undercutting of the material under the photoresist could occur on the leading wafer(s). Etch time varied by approximately 20-30% across a wafer.

#### IV. SHEET RESISTANCE OF IMPLANT DOPED SIPOS

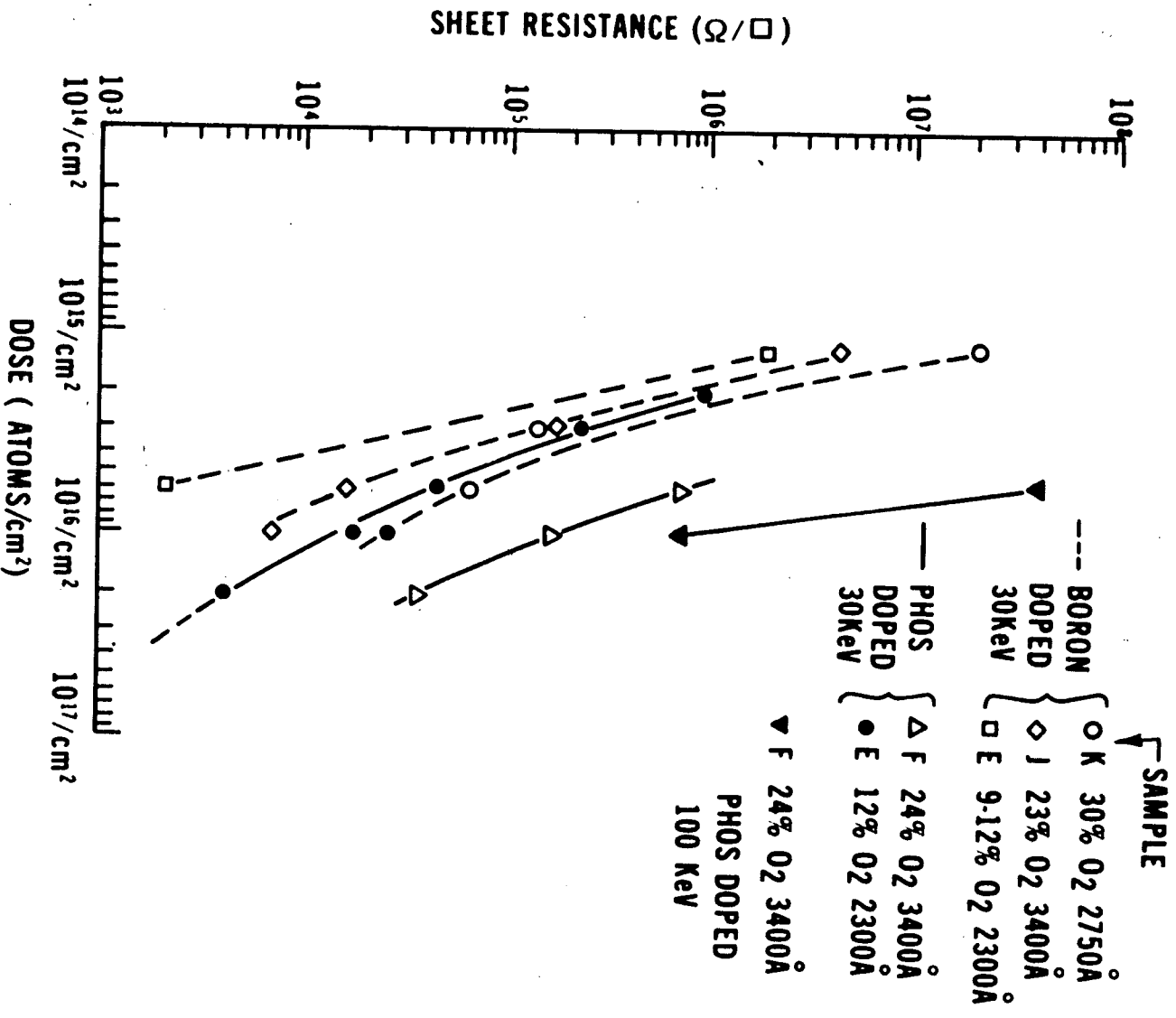
Figure 4 contains the measured sheet resistance dependence of SIPOS on impurity doping (boron and phosphorus) and the sheet resistance dependence of SIPOS on oxygen concentration. As the atomic percent of oxygen increases, the sheet resistance also increases for the range of implant doses shown in the figure. As the ion implant dose increases, the sheet resistance decreases.

The sheet resistance was measured using a four-point probe and fairly good agreement was achieved between the actual fabricated resistor and the four-point probe measurement for phosphorus doped films. For boron doped films, a significant difference exists between the four-point probe measurement and the actual fabricated resistors. These results are shown in Table 2. The resistance values of phosphorus doped resistors are about 25% below the values expected from four-point probe measurements. However, the boron doped resistors are as much as a factor of ten lower than the value expected from four-point probe measurements.

Figure 5 shows the four-point probe values after a one-hour 900°C anneal and the resistor values graphed alongside one another for the boron doped SIPOS. The difference exhibited between the two curves is caused by the subsequent heat treatments and processing which are dissimilar for the four-point probe film and the completed resistor structure. The completed resistor structure receives



**SHEET RESISTANCE VS IMPLANT DOSE  
FIGURE 4**

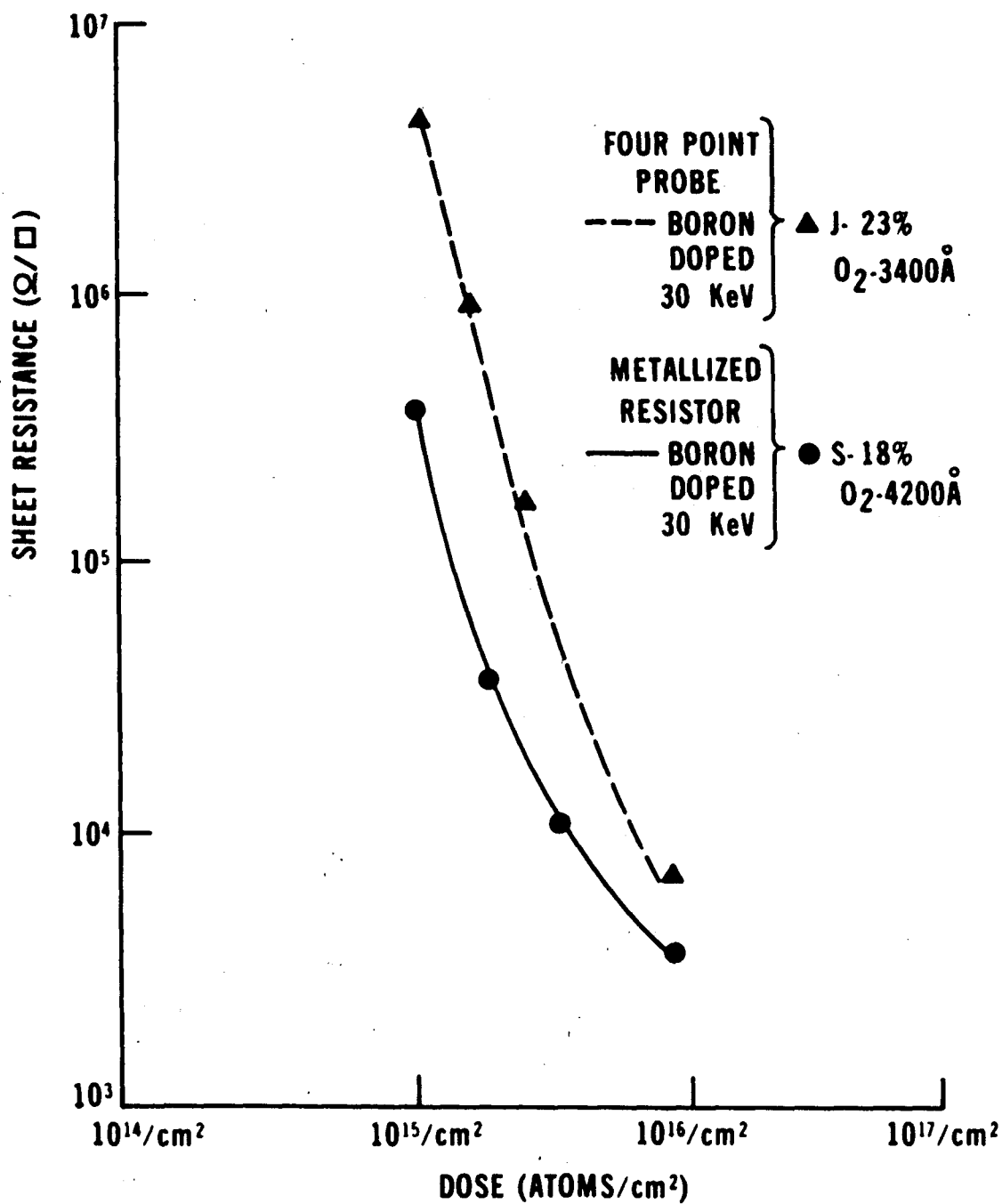


SHEET RESISTANCE VS IMPLANT DOSE  
FIGURE 4

**TABLE 2**  
**SHEET RESISTANCE**

<u>SLICE NO.</u>	<u>DOPANT</u>	<u>FOUR- POINT PROBE*</u>	<u>METALIZED RESISTOR</u>	<u>DOSE/CM<sup>2</sup></u>
R13	Phos.	62 K $\Omega$ /□	46.9 K $\Omega$ /□	1.5x10 <sup>16</sup>
R14	Phos.	62 K $\Omega$ /□	44.1 K $\Omega$ /□	1.5x10 <sup>16</sup>
R3	Boron	50 K $\Omega$ /□	11.7 K $\Omega$ /□	4x10 <sup>15</sup>
R5	Boron	50 K $\Omega$ /□	11.1 K $\Omega$ /□	4x10 <sup>15</sup>
S4	Boron	5 M $\Omega$ /□	360 K $\Omega$ /□	1.2x10 <sup>15</sup>
S14	Boron	500 K $\Omega$ /□	33.5 K $\Omega$ /□	2.2x10 <sup>15</sup>
S22	Boron	50 K $\Omega$ /□	10.4 K $\Omega$ /□	4x10 <sup>15</sup>
S34	Boron	5.6 K $\Omega$ /□	3.6 K $\Omega$ /□	1x10 <sup>16</sup>

\*Films were annealed for 1 hour at 900°C in nitrogen.



RESISTANCE OF SIPOS FILM  
FIGURE 5

approximately 90 minutes of high temperature processing after the deposited oxide step whereas the four-point probe film receives 60 minutes. Redistribution of the doping, doping activation, different phase compositions and different grain sizes of the film may occur causing this discrepancy. Also the difference in atomic % oxygen caused some of the change noted. Interestingly, as the doping is increased, the two curves in Figure 5 approach one another in terms of their electrical resistivity; this may be due to saturation of the doping activation. From the data in Table 2, one also notes that a  $1 \times 10^{16}/\text{cm}^2$  boron doped resistor is low by .36% and a  $1.5 \times 10^{16}/\text{cm}^2$  phosphorus doped resistor is low by .27%, hence suggesting the saturation of doping activation at higher dose concentrations.

The sheet resistance of implant doped SIPOS films is very critically sensitive to the implant dose and virtually no conduction ( $> 4 \times 10^7 \Omega/\square$  sheet resistance) occurs for 3000Å thick films implanted at 30 KeV with doses less than  $6 \times 10^{14}/\text{cm}^2$  of boron. Also virtually no conduction ( $> 4 \times 10^7 \Omega/\square$  sheet resistance) occurs for 30 KeV phosphorus implant doses of less than  $1 \times 10^{15}/\text{cm}^2$  as shown in Figure 4. The critical sensitivity of the sheet resistance to implant dose can be seen by looking at the boron doped 23% oxygen curve in Figure 5. The sheet resistance drops approximately two decades of resistance for one decade increase of implant dose for the boron doped annealed resistors. A very complex mechanism of impurity redistribution is probably occurring due to several known phenomena.

The SIPOS<sup>18</sup> film which consists of silicon, oxygen and impurity atoms is amorphous after deposition. During the heat treatments that follow SIPOS deposition, the film goes from an amorphous state into polycrystalline silicon and silicon oxide phases causing the physical thickness of the film to shrink by ~10%. As the heat treatment proceeds, crystallites (or grains) are formed each incorporating some of the impurity atoms with the remainder of the impurity atoms being incorporated between crystallites (in the grain boundary). At this point both grain and grain boundary diffusion occur. The diffusion coefficient for phosphorus in the SiO<sub>2</sub> species of the SIPOS film is much larger than the diffusion coefficient for boron. In the Si species of the SIPOS film a similar diffusion coefficient is obtained for both boron and phosphorus. In the grain boundary a different coefficient exists which is large for low temperatures. The segregation coefficient which gives a measure of the impurity redistribution at the silicon/silicon dioxide interface on crystallographic silicon is .3 and 10 for boron and phosphorus respectively. This provides some of the additional reasons for the different resistivities obtained for similar doses and depth of boron and phosphorus impurities.

A comparison of phosphorus doped SIPOS at 30 keV and 100 keV implant energies indicates that the sheet resistance is increased by using the higher energy as shown in Figure 4. Comparing boron doped SIPOS at 30 keV implant energy to phosphorus at 100 keV implant



energy, one notes that they both have similar depths into an  $\text{SiO}_2$  or Si film (and thus SIPOS too) according to the projected range statistics. However, as shown in Figure 4, phosphorus doped SIPOS is more resistive for a given implant dose. Again these effects may be due to the complex diffusion in SIPOS and may depend on the anneal time and temperature.

From the first four SIPOS runs used to characterize the film, a mean of 23 atomic % oxygen was achieved with a standard deviation of  $\pm 3\%$ . From Figure 4, a  $\pm 3\%$  variation of oxygen content for the  $4 \times 10^{15}/\text{cm}^2$  boron dose gives approximately a 100% variation in the range of sheet resistance. The ion-implant dose which can be controlled to approximately  $\pm 3\%$  gives about a 50% variation of the sheet resistance.

## V. RESISTOR PROPERTIES

Several resistor properties were measured on both doped films and on metalized resistor structures. Contact resistance, temperature coefficient of resistance and resistor linearity with applied voltage were measured since they were considered to be most important.

### A. CONTACT RESISTANCE OF SIPOS RESISTORS

Contact resistance of the SIPOS resistors can be calculated from the following formulas:

$$R = 2R_c + NR_{\square}$$

$$R_c = \frac{R - NR_{\square}}{2}$$

where

$R_c$  = contact resistance ( $\Omega$ )

$N$  = number of squares ( $\square$ )

$R_{\square}$  = sheet resistance in ( $\Omega/\square$ )

$R$  = resistance ( $\Omega$ )

$R$  is the measured resistance in the linear portion of the current-voltage trace. One can calculate both the contact resistance and the sheet resistance by measuring two resistors ( $R_1$  and  $R_2$ ) of different but known length ( $N_1$  and  $N_2$ ). Then one only needs to solve the simultaneous equations for  $R_c$  and  $R$ . Thus,

$$R_c = \frac{1}{2} \left( \frac{N_2 R_1 - N_1 R_2}{N_2 - N_1} \right),$$

where  $R_1$  and  $R_2$  are the measured resistance values.

The contact resistance is dose and dopant dependent and provides a sheet resistance of .4 and .5 squares for phosphorus and .7 and .8 squares for boron for the doses shown in the following table. We can also see from the following table that the average contact resistance ( $\bar{R}_c$ ) increases as the implant dose is decreased for a particular dopant.

<u>DOPANT</u>	<u>SLICE</u>	<u><math>\bar{R}_c</math></u>	<u>SHEET RESISTANCE</u>	<u>IMPLANT DOSE/cm<sup>2</sup></u>	<u><math>\bar{R}_c</math> / SHEET RESISTANCE</u>
Boron	R5	22.5K $\Omega$	28K $\Omega$	4x10 <sup>15</sup>	.8
Boron	R9	38.7K $\Omega$	58K $\Omega$	3x10 <sup>15</sup>	.7
Phosphorus	R14	27K $\Omega$	61K $\Omega$	1.5x10 <sup>16</sup>	.44
Phosphorus	R19	54.9K $\Omega$	112K $\Omega$	1x10 <sup>16</sup>	.49

#### B. TEMPERATURE COEFFICIENT OF RESISTANCE

Temperature coefficient of resistance (TCR) measurements were made on films of 12% oxygen concentration SIPOS doped with boron. These measurements were obtained by placing two probes approximately a centimeter apart onto the film and measuring the resistance while the slice was in an oven. Measurements were made with very light pressure gold wire probes to avoid contact pressure errors as shown in Figure 6. The 6x10<sup>15</sup>/cm<sup>2</sup> dose film gave a TCR of +705 ppm/°C.

## **SENSITIVITY OF SIPOS RESISTIVITY TO VARIOUS PROBE PRESSURES**

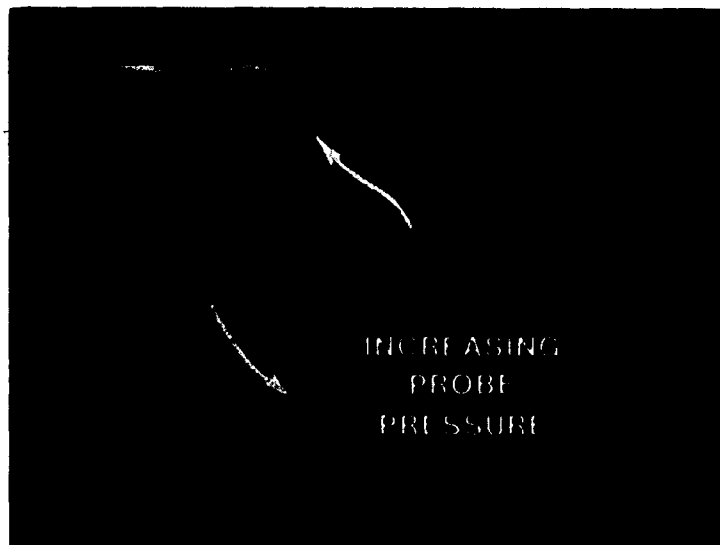


**FIGURE 6**

Compared to diffused resistors, this is an excellent value. Diffused resistors typically have values of approximately 1800 ppm/°C and pinch resistors are even higher.

### C. LINEARITY OF SIPOS RESISTORS

The linearity of SIPOS resistors is a function of the applied electric field and doping concentration. A study of six resistors, which are heavily doped ( $1.5 \times 10^{16}/\text{cm}^2$  phosphorus), all having 75 $\mu\text{m}$  lengths and varying in width from 5 $\mu\text{m}$  to 30 $\mu\text{m}$  showed that the resistors are linear for electric fields  $\leq 2\text{KV}/\text{cm}$ . For electric fields of 6KV/cm, the resistance decreases by 10% for 5 $\mu\text{m}$  resistor widths. However, for the 10 $\mu\text{m}$  to 30 $\mu\text{m}$  range of widths and at an electric field of 6KV/cm, the resistance decreases by about 5%. Further investigation revealed a processing anomaly which causes the resistor body near the contact end to widen on all resistors, but does not significantly affect the overall resistance except on narrow resistor widths (5 $\mu\text{m}$ ). This accounts for the increase in resistance noted on the 5 $\mu\text{m}$  resistors and is described further in Section VII B.

Undoped SIPOS is virtually nonconductive ( $10^{10}$ – $10^{18}$   $\Omega/\square$ ) at low electric fields. Lowly doped SIPOS exhibits a bimodal conduction behavior simulating that of a reverse breakdown characteristic of a diode. Both high and low doping concentration effects on the SIPOS resistors are described in the next section.

## VI. ELEMENTARY PHYSICS OF IMPLANTED SIPOS RESISTOR STRUCTURES

Experimentally, SIPOS films implanted with doses of  $10^{12}/\text{cm}^2$  to  $10^{14}/\text{cm}^2$  exhibit a conduction behavior resembling that of a diode in reverse breakdown as mentioned in the previous section and as shown in Figure 7. Annealing for periods of one hour at  $900^\circ\text{C}$  or  $1000^\circ\text{C}$  does not affect the breakdown characteristic significantly. However, annealing at  $1100^\circ\text{C}$  causes the breakdown characteristic to soften. Doses between  $10^{15}/\text{cm}^2$  to  $10^{16}/\text{cm}^2$  exhibit nearly linear characteristics. Thus both conduction and breakdown mechanisms of electrical transport occur in impurity doped SIPOS films. For implant doses  $\leq 10^{14}/\text{cm}^2$  ( $\leq 3 \times 10^{19}/\text{cm}^3$  concentration), a diode breakdown characteristic is observed. At some critical dose  $\geq 10^{14}/\text{cm}^2$  ( $\geq 3 \times 10^{19}/\text{cm}^3$  concentration), linear conduction occurs as shown in the lower half of Figure 8 and is ohmic up to doses of  $10^{16}/\text{cm}^2$ . The above doses were implanted at an energy of 30 keV.

### A. HIGH CONCENTRATION REGION

The high concentration region ( $\geq 3 \times 10^{19}/\text{cm}^3$ ) provides nearly linear resistors as shown in the current-voltage characteristic of Figure 8 after the one-hour  $900^\circ\text{C}$  anneal of the polysilicon to SIPOS contact. Without an anneal the films exhibited a nonlinear behavior at the origin; the nonlinearity is suspected to be caused by an interfacial oxide and/or lack of doping activation.

SIPOS is essentially an amorphous material as deposited. After annealing, grains begin to form in the material. Like polysilicon,

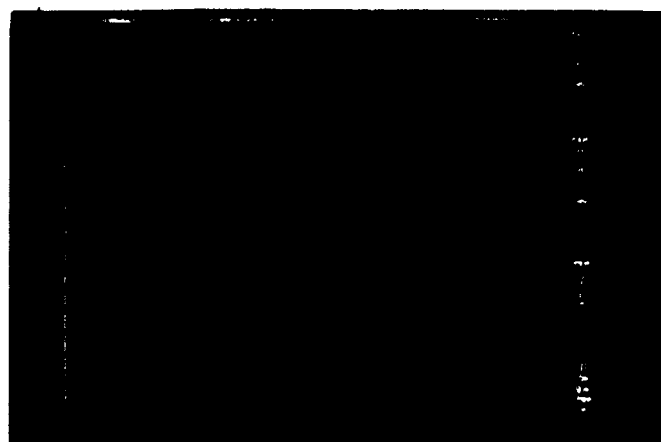


DOSE—  $10^{14}/\text{cm}^2$

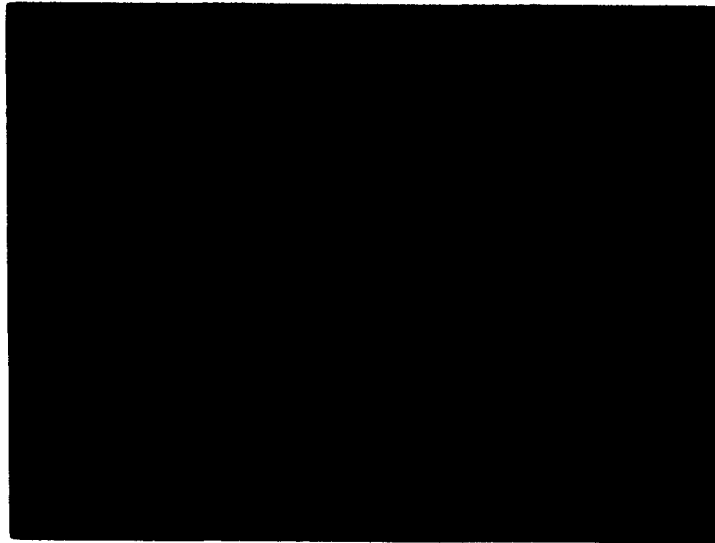


DOSE—  $10^{13}/\text{cm}^2$

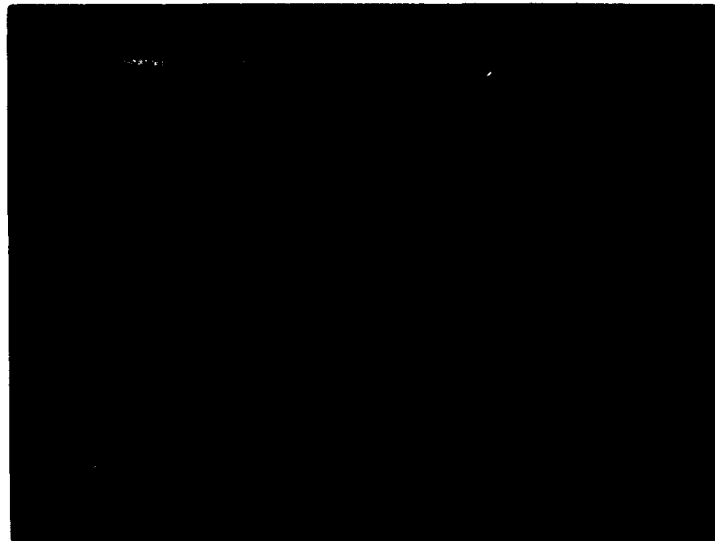
DOSE—  $10^{12}/\text{cm}^2$



**CURRENT-VOLTAGE SLOPE DEPENDENCE ON IMPLANT DOSE**  
**FIGURE 7**



**BEFORE ANNEAL**



**AFTER ANNEAL FOR 1 HOUR  
AT 900°C IN NITROGEN**

**LINEARITY OF A BORON DOPED 19% OXYGEN  
CONCENTRATION SIPOS RESISTOR**

**FIGURE 8**



it can be treated physically as a network of crystallites doped with oxygen and boron or phosphorus. Thus it obeys polysilicon type conduction models.

A carrier-trapping model<sup>9,10,11,12,13</sup> has been used to explain the conduction behavior of doped polysilicon and this model appears to fit the conduction behavior noted in SIPOS. The model predicts grain boundary trapping states which trap part of the thermally ionized carriers. Hence the number of carriers is reduced and a potential barrier impeding carrier flow from crystallite to crystallite is generated. At high doping levels the potential barrier is easily tunneled through, causing the semiconducting action to be degenerate and allowing nearly ohmic behavior of the material.

#### B. LOW CONCENTRATION REGION

In the low concentration region ( $< 3 \times 10^{19}/\text{cm}^3$ ), nearly 250 volts must be applied to a .240 $\mu\text{m}$  long resistor (or an electric field of  $10^4 \text{ V/cm}$ ) before any conduction occurs. At this point, breakdown of the film occurs and the slope of the current-voltage trace in breakdown becomes nearly ohmic and dependent on the implant dose (see Figure 7).

According to the carrier-trapping model,<sup>9,10,11,12,13</sup> the potential barrier impeding carrier flow from crystallite to crystallite is not that of a degenerate semiconductor at these doping concentrations and must be overcome by approximately 1 volt/ $\mu\text{m}$  field before conduction occurs. Once this potential barrier is overcome,

then breakdown of the film occurs and the doping concentration in the grain determines the resistance of the current voltage characteristic shown in Figure 7.

### C. POLYSILICON AND SIPOS SIMILARITIES AND DISSIMILARITIES

The conduction behavior of SIPOS and POLYSILICON appear to be similar in that polysilicon exhibits the critical dependence of the sheet resistance on implant dose as shown in Figure 9.<sup>14</sup> Polysilicon resistivity drops rapidly in the dose range of  $10^{13}/\text{cm}^2$  to  $10^{14}/\text{cm}^2$  while SIPOS requires doses in the  $10^{15}/\text{cm}^2$  to  $10^{16}/\text{cm}^2$  range before significant conductivity is obtained. Both polysilicon<sup>15</sup> and SIPOS can provide resistors of short lengths. See Figures 10 and 11. However, short length resistors ( $5\mu\text{m}$  to  $20\mu\text{m}$  length) are susceptible to electrical burnout from voltage transients.

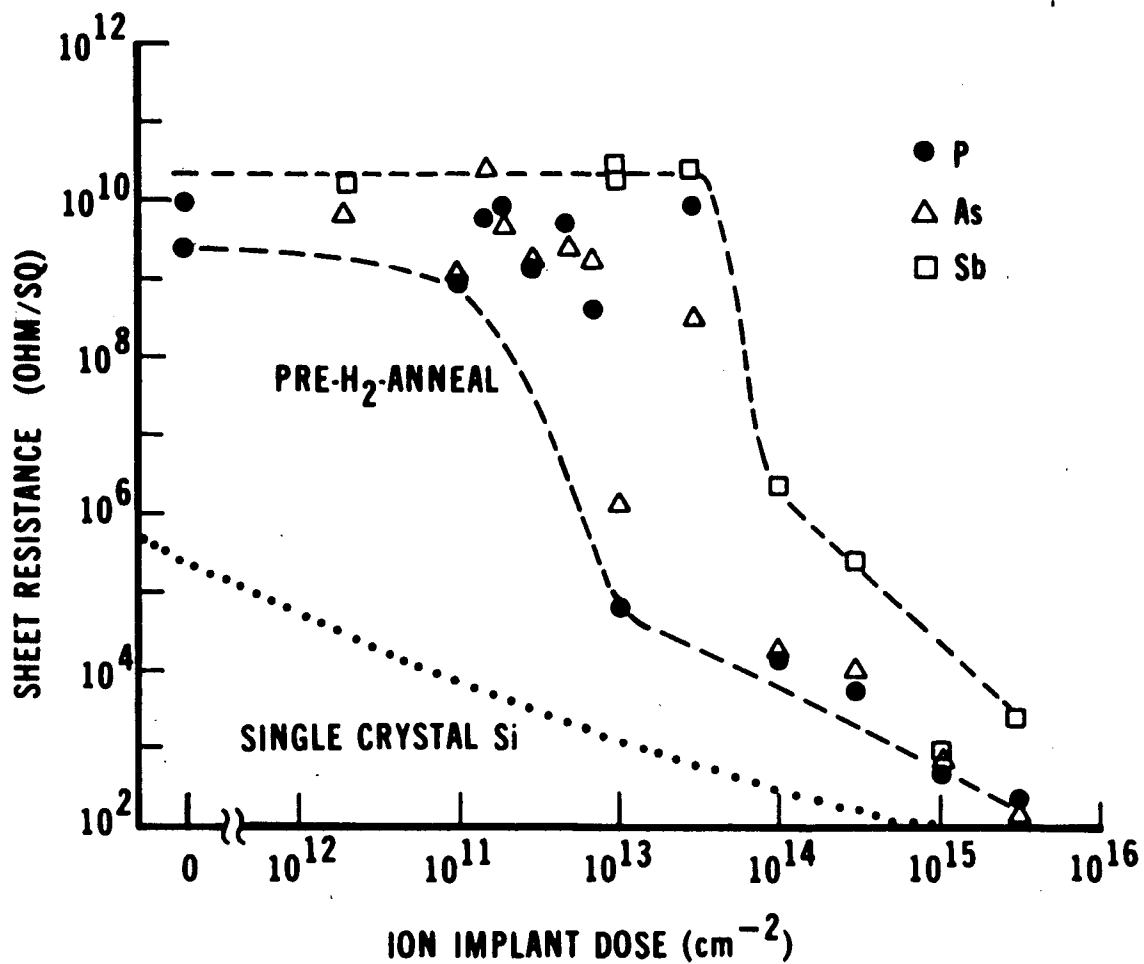
Gerzberg<sup>9,16</sup> studied the transport mechanism in polysilicon and concluded that the conduction of polysilicon is limited by the thermionic emission of majority carriers. He concluded that the current-voltage behavior of polysilicon obeys the following formula:

$$I = AJ = 2K \sinh \frac{q V_g}{2 kT}$$

A is area of the conduction portion of polysilicon film

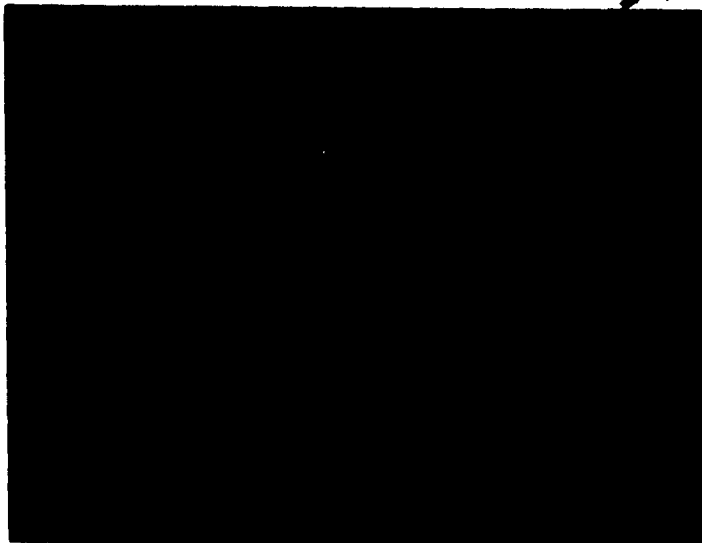
J is current density

$V_g$  is voltage across a grain

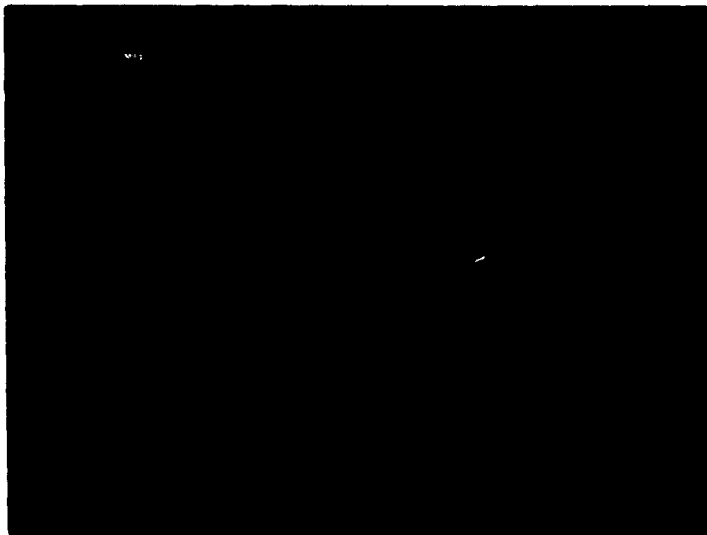


RESISTANCE OF IMPLANTED POLY-Si

FIGURE 9



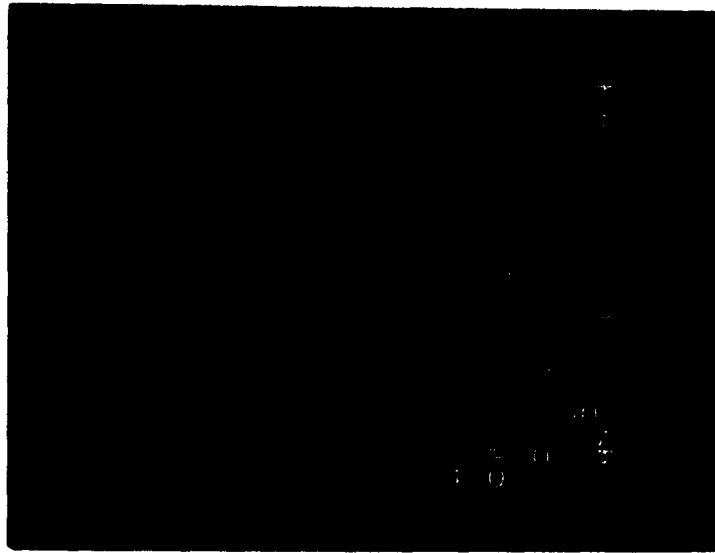
**5 $\mu$  LENGTH**



**10 $\mu$  LENGTH**

**POLYSILICON RESISTORS  
HAVING SHORT LENGTHS**

**FIGURE 10**



**"A"**

**20 $\mu$  to 400 $\mu$  LENGTH**



**"B"**

**5 $\mu$  LENGTH**

**VARIOUS RESISTOR LENGTHS**

**FIGURE 11**

$$K = AA^* T^2 \exp \left( \frac{-q V_B}{kT} \right)$$

$A^*$  is the Richardson constant ( $\approx 120 \text{ A/cm}^2 \text{ } ^\circ\text{K}^2$ )

$V_B$  is the potential barrier

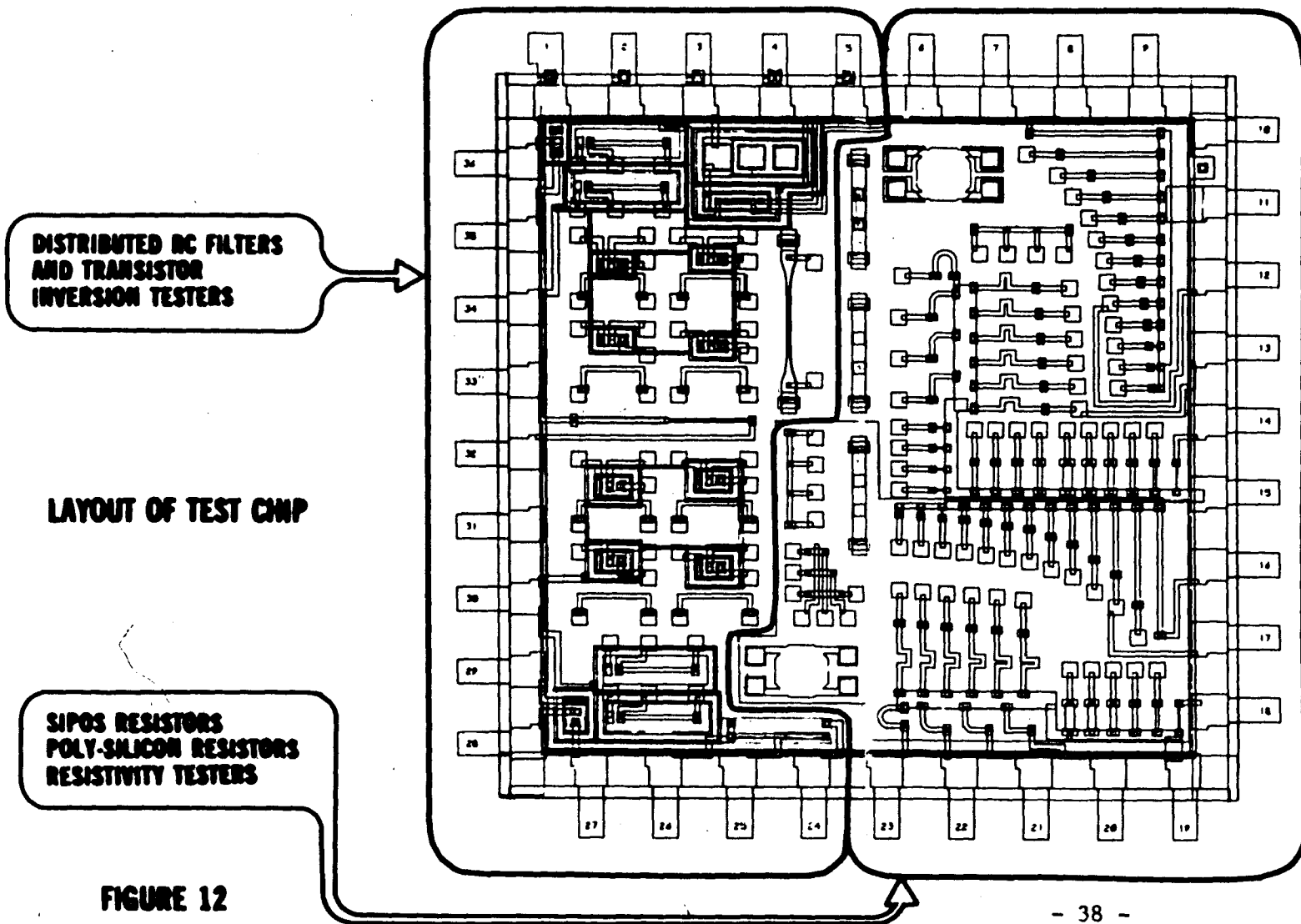
Figure 11A shows the I-V behavior for a family of SIPOS resistors ranging from 20 $\mu\text{m}$  to 400 $\mu\text{m}$  in length plus a single 5 $\mu\text{m}$  long resistor in Figure 11B. The nonlinearity due to high electric fields is apparent on the 5 $\mu\text{m}$  resistor and the magnitude of the electric field is indicated on the abscissa. The SIPOS resistance behavior for the high dose region looks like the hyperbolic sine function and appears to obey similar transport mechanisms as polysilicon.

## VII. RESISTOR TEST PATTERN

A test pattern to study SIPOS resistors was developed and is shown in Figure 12. In general, the SIPOS resistor test pattern is laid out in two sections. One section is comprised of the SIPOS resistors, polysilicon resistors and the resistivity testers. The other section is comprised of the distributed RC electrical filters and transistor inversion testers. A list of the elements on the test pattern is given in Figure 13 and includes resistors, electrical filters, transistors and resistive crossovers. Varying lengths, widths, meanders and end contact size test resistors were fabricated and are detailed in Figures 14, 15, 16 and 17. Several low pass filters and one high pass filter were fabricated with the assumption that doped SIPOS could be represented as only a resistive component in the structures. Diffused regions supplied other resistive material; also, deposited and grown oxides supplied the dielectric for the distributed capacitance of the RC filters. In addition, several inversion test structures were fabricated to investigate the possibility of inversion effects over the diffused isolation areas of standard transistors. Due to a time limitation, only the SIPOS resistors were processed and examined in detail.

### A. TEST PATTERN ELEMENTS

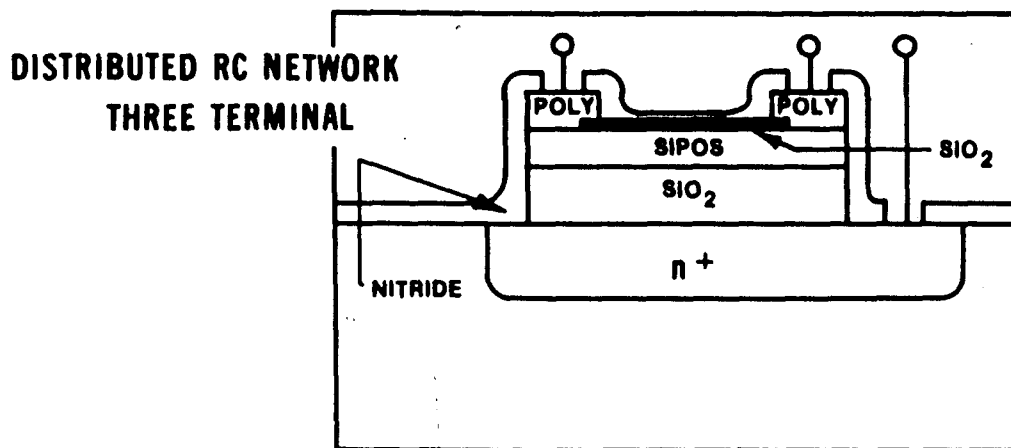
The topography of four sets of resistors is shown in Figures 14-17. The dashed area is the region that is metalized on the structure. In Figure 14, the size of the polysilicon connecting





## RESISTORS

1. VARIOUS LENGTHS OF RESISTORS WITH FIXED WIDTH
2. VARIOUS WIDTHS OF RESISTORS WITH FIXED LENGTH
3. VAN DER PAUW PATTERNS
4. MATCHED RESISTORS AND RATIOS OF RESISTORS
5. EXPERIMENTAL TYPES OF MEANDERS
6. EXPERIMENTAL RESISTOR END CONNECTIONS
7. EXPERIMENTAL BENDS



## TRANSISTORS

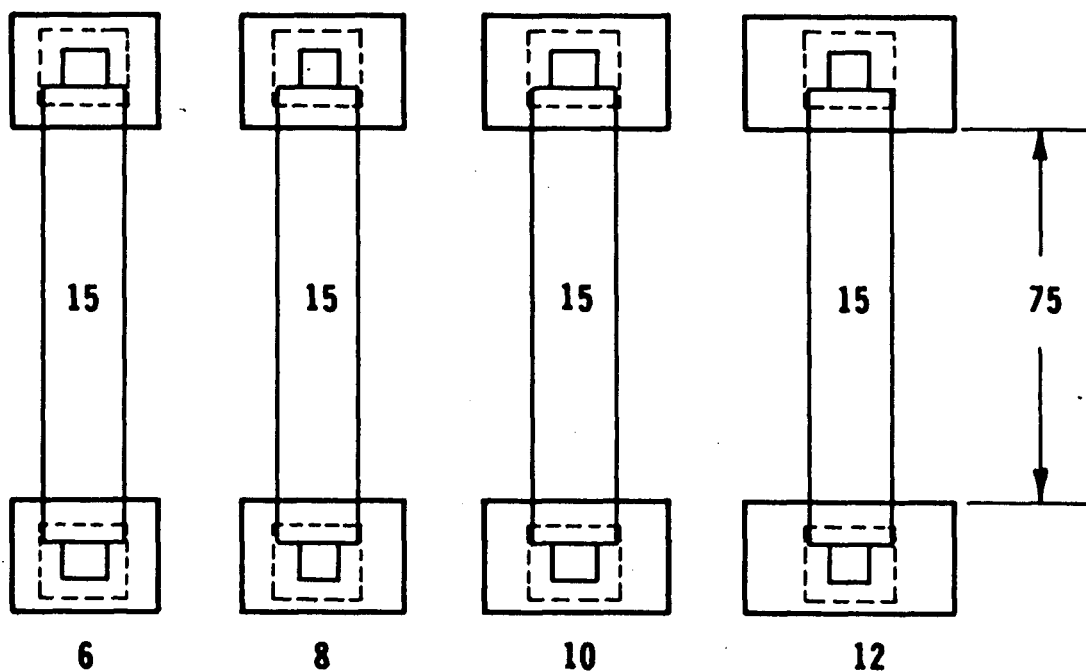
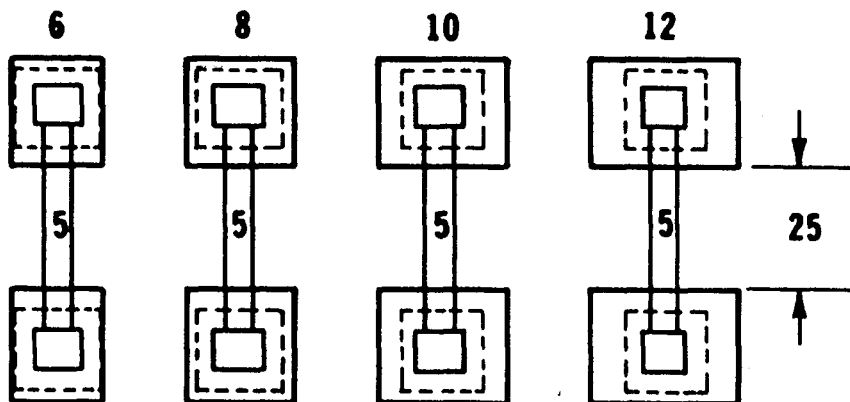
STANDARD NPN AND PNP

RESISTIVE CROSSOVER (WITH POLY Si)

SINGLE, DOUBLE, TRIPLE

## ELEMENTS OF TEST PATTERN

FIGURE 13



**SIPOS RESISTORS**  
**RESISTOR END CONTACT TEST**

**FIGURE 14**

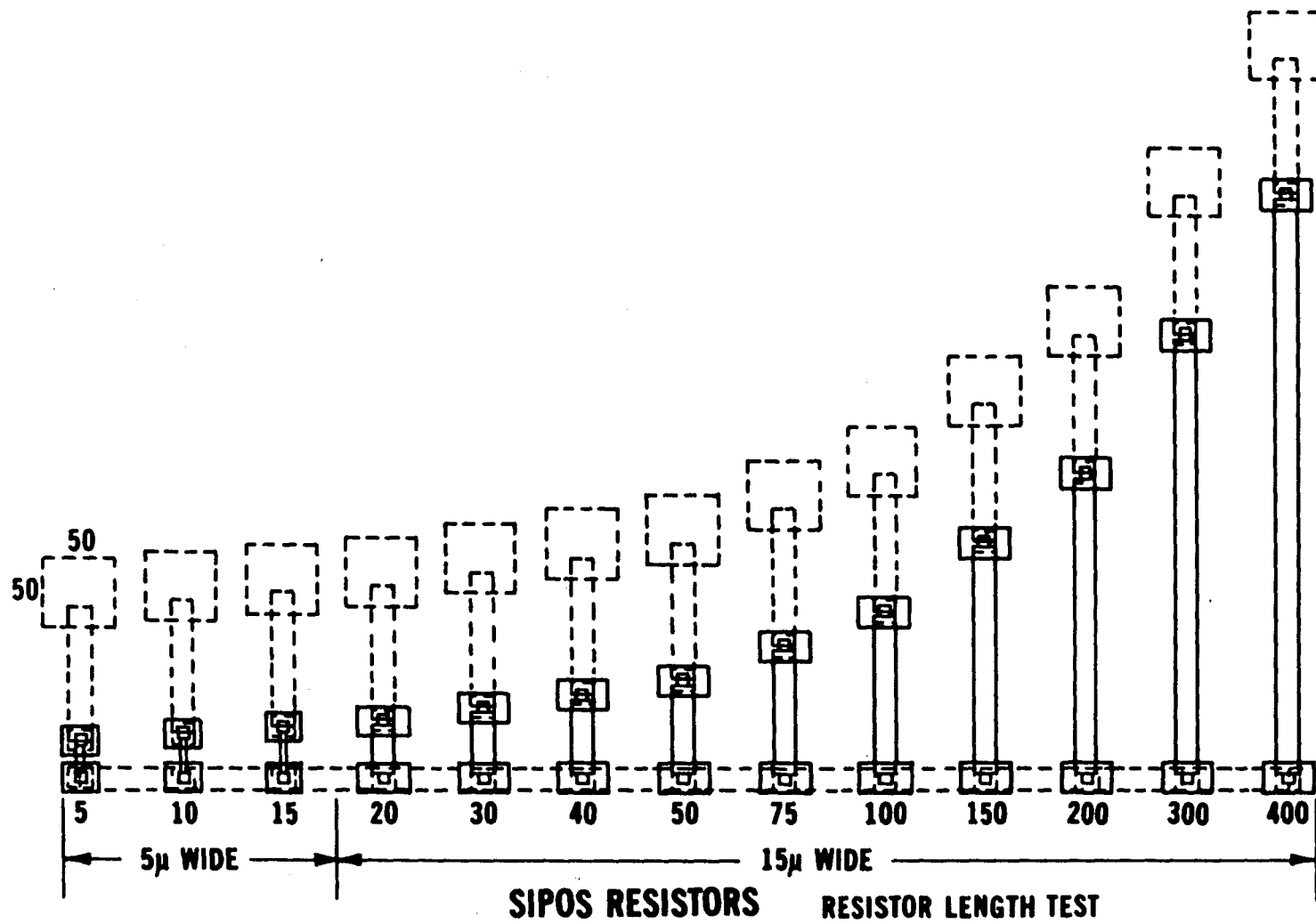
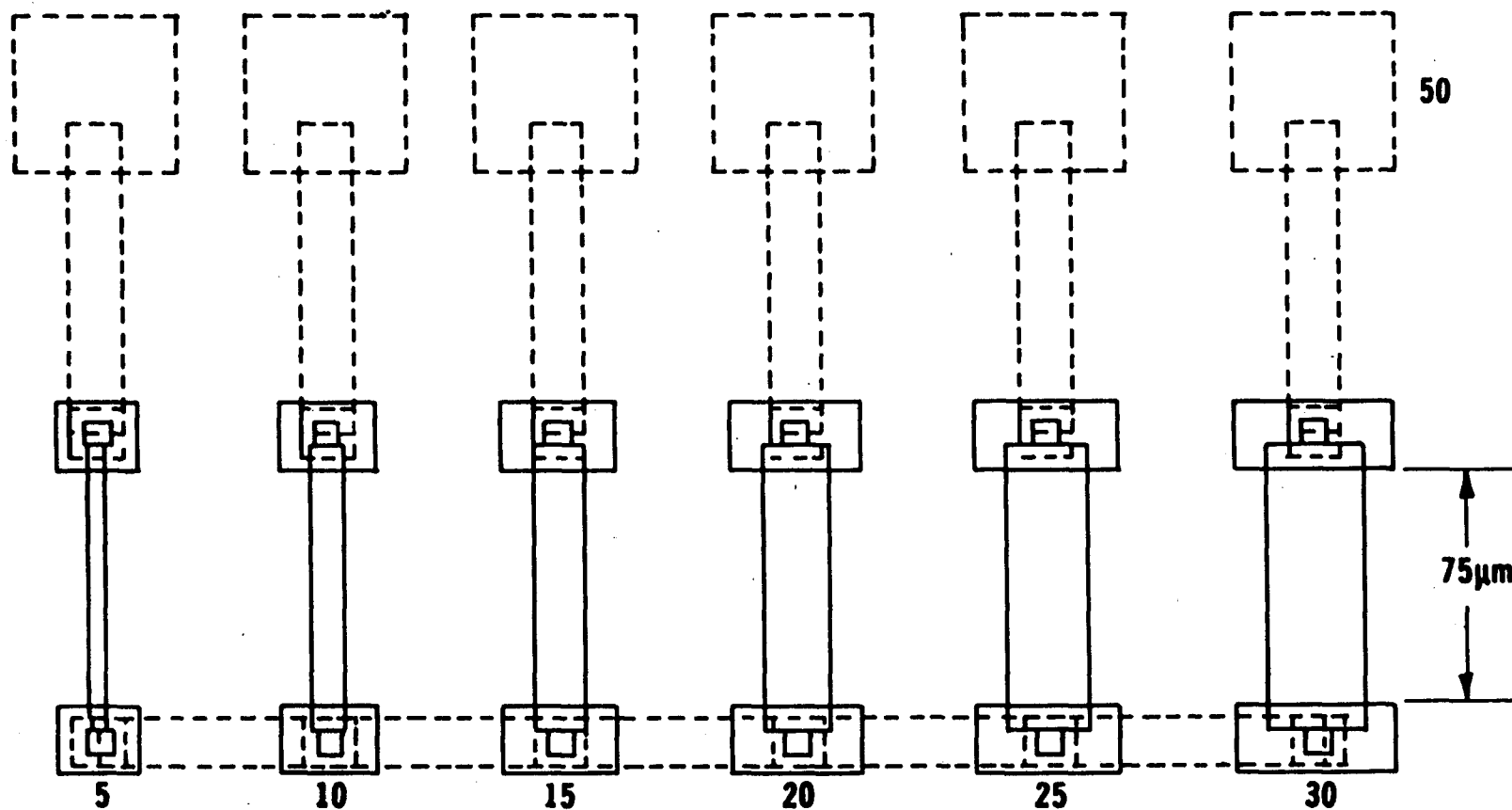
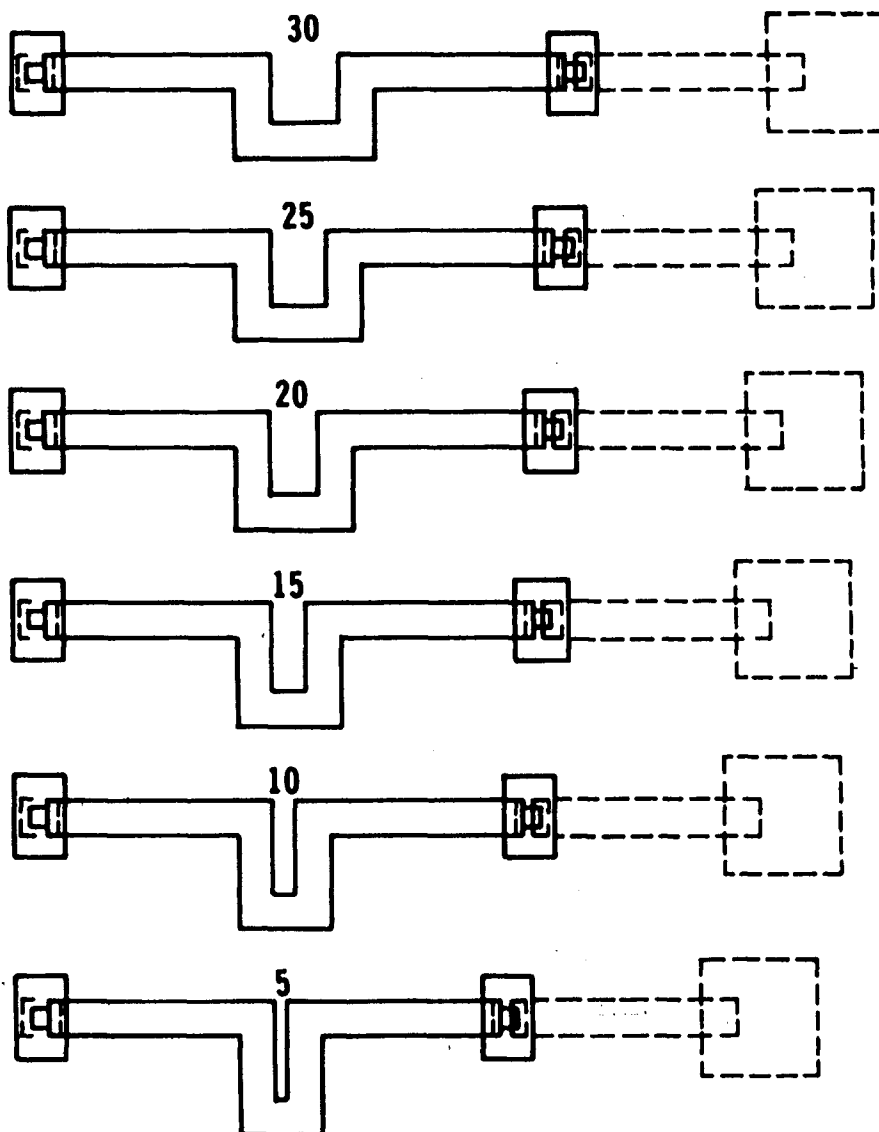


FIGURE 15



**SIPOS RESISTORS**  
**RESISTOR WIDTH TEST**  
**FIGURE 16**



**SIPOS RESISTORS**  
**RESISTOR MEANDER TEST**

**FIGURE 17**

pad is varied for two different resistor widths ( $5\mu\text{m}$  and  $15\mu\text{m}$ ) to study contact resistance variation with connecting pad size.

Figure 15 depicts resistor lengths from  $5\mu\text{m}$  to  $400\mu\text{m}$  with two different width variations:  $5\mu\text{m}$  and  $15\mu\text{m}$ . Figure 16 shows the variations of both the polysilicon connecting pad and the resistor width while Figure 17 shows the variations of the resistor meander but maintains the same number of squares of resistance.

Four distributed RC networks were fabricated on the test chip of the form shown in Figure 13. The SIPOS was made of a common length for the networks and the dielectric thickness underneath was varied by putting the SIPOS resistor over four oxidized areas of different thickness.

#### B. TEST PATTERN RESULTS

Devices were fabricated with resistors ranging from approximately  $5\text{K}\Omega$  to  $10\text{M}\Omega$  using the test chip showing in Figure 12. Both boron and phosphorus doped films were fabricated, although only boron resistors were made over the entire range indicated. Due to a time limitation, only the resistors and the resistive crossovers were fabricated; no RC filters and no transistor inversion structures were processed. The resistor end contact test showed that enlargement of the contact width by a factor of 2 lowered the resistance by only 2% for  $5\mu\text{m}$  wide resistors. Enlargement of the contact width for the  $15\mu\text{m}$  wide resistors showed no significant decrease in the resistance. From the resistor length test, the electric field dependence of

resistor linearity was discovered, as discussed earlier. The resistor width test showed that the calculated sheet resistance varies by 10% over the resistor width range of 5 $\mu$ m to 30 $\mu$ m. Over the resistor width range of 10 $\mu$ m to 30 $\mu$ m, the calculated sheet resistance varies by 5%. Since the resistors are located all within several hundred microns of one another, the actual doping of the SIPOS film should be quite similar and one would expect the sheet resistance to be similar between the resistors. The discrepancy results from an underetching variation which causes the resistor width near the connecting pad to be wider than the main body and hence be noticeable in narrow resistors as shown in Figure 18. The resistor meander test had loops varying from 5 $\mu$ m to 30 $\mu$ m in width. The test results indicate that the same resistance was obtained for the 10 $\mu$ m to 30 $\mu$ m wide loops, but the 5 $\mu$ m wide loop resistor was low by 2.5% due to a processing anomaly in which the processed resistor body was rounded at the meander as shown in Figure 19.



**PROCESSING ANOMALY CAUSES WIDENING  
OF RESISTOR BODY NEAR CONTACT END**



**WIDENING EFFECT OF  
RESISTOR BODY NEAR CONTACT END**

**FIGURE 18**





**ROUNDING EFFECT OF  
5 $\mu$ m RESISTOR MEANDER**



**ROUNDING EFFECT OF RESISTOR MEANDER**

**FIGURE 19**

### VIII. CONCLUSIONS

A linear integrated circuit process has been modified to provide oxide isolated resistors having high sheet resistance, polysilicon crossovers and distributed RC electrical filters. This was accomplished by developing an addition to the process which utilizes two photoresist steps plus polysilicon, SIPOS and oxide depositions. The resistor body is composed of SIPOS doped by ion implantation and is contacted by two polysilicon pads. Sheet resistances in the range of  $3.6\text{K}\Omega/\square$  to  $360\text{K}\Omega/\square$  were obtained with the designed structure. Distributed RC electrical filters were designed to use SIPOS as a resistive-only component and to use the oxide under the SIPOS as the dielectric for the capacitance. The silicon and SIPOS formed the plates of the capacitor. The dielectric thickness was varied by depositing the SIPOS over thicker or thinner oxides of the silicon chip. Additional studies of the electrical filters and the polysilicon crossovers will supply information on their utility.

Test patterns were designed to study the geometric effects of processing on the final resistor. The resistor end contact tester showed that enlargement of the end contact width by a factor of 2 lowered the resistance by only 2% which is not significant. The resistor meander test revealed that resistor meanders that are  $5\mu\text{m}$  wide do affect the final sheet resistance due to a rounding effect of the processed body of the resistor while meanders greater than or equal to  $10\mu\text{m}$  spacing do not affect the resistance. The resistor

width test revealed an anomaly which causes 10% variation of the effective sheet resistance over the 5 $\mu$ m to 30 $\mu$ m resistor width range. Undercutting was observed which caused the resistor width to be widened near the contacts and affected the sheet resistance of the 5 $\mu$ m length resistor significantly.

The test pattern resistors and doped films were examined to study resistor linearity, contact resistance, resistor reproducibility and TCR behavior. Linearity of the SIPOS resistor structure was found to be dependent on both implant dose and on the electric field applied across the finished resistor. For implant doses of  $\leq 10^{14}/\text{cm}^2$ , the structure exhibited a bimodal conduction resembling a diode under reverse bias. For implant doses above the critical dose, SIPOS resistors are linear up to electric fields of 2KV/cm and decrease in resistance by 10% or less for electric fields up to 6KV/cm. Contact resistance was found to be dose dependent and typically varied between 0.5 and 1.0 square of sheet resistance. Preliminary measurement of the temperature coefficient of resistance on a 12% oxygen concentration film yielded 705 ppm/ $^{\circ}$ C. Resistor reproducibility was found to be very sensitive to oxygen content and ion implant dose variations as well as anneal conditions. A  $\pm 3\%$  oxygen content variation yielded a 100% sheet resistance variation. And a  $\pm 3\%$  ion implant dose variation yielded 50% variation in the sheet resistance. Combining the results of sheet resistance, contact resistance, electric field dependence and TCR behavior, the

equivalent resistance for a given dose, oxygen content and fixed voltage would be:

$$R_{\text{equivalent}} = 2R_c + NR_{\square} - R_e + R_{\text{TCR}}$$

where

$R_c$  = the contact resistance ( $\Omega$ )

$N$  = the number of squares ( $\square$ )

$R_{\square}$  = the sheet resistance ( $\Omega/\square$ )

$R_e$  = the electric field dependence of resistance ( $\Omega$ )

$R_{\text{TCR}}$  = the temperature behavior of resistance ( $\Omega$ ).

A significant difference in sheet resistance was obtained between the four-point probe measurement and the calculation from a metalized resistor as shown in Figure 5. The difference exhibited between the two curves is caused by the subsequent heat treatments and processing which are dissimilar for the four-point probe film and the completed resistor structure. The very complex mechanism of impurity redistribution, different phase compositions, doping activation and different grain sizes of the film all contribute to the difference noted.

SIPOS and polysilicon obey similar transport phenomena in that both exhibit a critical dependency of sheet resistance on dose. Polysilicon obeys the carrier trapping model and SIPOS appears to also obey this model. Since the test structures were only tested under direct current conditions, the effects of carrier trapping

should be investigated to see if the linear resistive mode exhibits any frequency dependence.

Assuming the linear mode is not affected significantly by frequency, the implant doped SIPOS resistor should be useful in circuit applications which can tolerate 100% to 150% sheet resistance variability. Circuit applications which require high sheet resistance, high voltages per unit length and/or oxide isolation are especially suited to the doped SIPOS process. Additional measurements of the temperature coefficient of resistance would supply information on how the actual resistor structure behaves with temperature since the TCR measurements described earlier were made only on a SIPOS film and not on the completed SIPOS resistor. Thermal aging with applied bias on the resistor would provide information on the stability of the resistor under operating conditions.

## REFERENCES

1. T. Aoki, T. Matsushita, H. Yamoto, H. Hayashi, M. Okayama and Y. Kawana, "Oxygen-doped Polycrystalline-Silicon Films Applied to Surface Passivation," Electrochem. Soc. Meeting, May 1975, Extended Abst. #148.
2. T. Matsushita, T. Aoki, T. Otsu, H. Yamoto, H. Hayashi, M. Okayama and Y. Kawana, "Highly Reliable High-Voltage Transistors by Use of the SIPOS Process," IEEE Trans. Elect. Dev., ED-23, 826 (1976).
3. H. Mochizuki, T. Aoki, H. Yamoto, M. Okayama, M. Abe and T. Ando, "Semi-Insulating Polycrystalline-Silicon (SIPOS) Films Applied to MOS Integrated Circuits," Suppl. J. J. Appl. Phys., 15 41 (1976).
4. H. Yamoto, N. Oh-uchi, H. Hayashi, T. Matsushita and Y. Kawana, "New Technology by Use of the Doped SIPOS Films," Extended Abst. #168, Electrochemical Society Meetings, May 1979.
5. D. J. Hamilton, W. G. Howard, Basic Integrated Circuit Engineering, McGraw Hill, 1975.
6. H. R. Camenzind, Electronic Integrated Systems Design, Van Nostrand Reinhold Company, 1972.
7. W. Jung, IC Op-Amp Cookbook, Howard W. Sams and Co. Inc., p. 498, 499.
8. W. S. Johnson and J. F. Gibbons, Projected Range Statistics in Semiconductors, Stanford California University Press, 1970.
9. N. C. C. Lu, L. Gerzberg, C. Y. Lu and J. D. Meindl, "Modeling and Optimization of Monolithic Polycrystalline Silicon Resistors," ELECTRON DEVICES, Vol. ED-28, No. 7, July 1981.
10. G. Baccarani, B. Ricco and G. Spadini, "Transport Properties of Polycrystalline Silicon Films," J. Appl. Phys. Vol. 49, 1978.
11. J. Y. W. Seto, "The Electrical Properties of Polycrystalline Silicon Films," J. Appl. Phys. Vol. 46, 1975.

12. N. C. C. Lu, L. Gerzberg, C. Y. Lu and J. D. Meindl, "A New Conduction Model for Polycrystalline Silicon Films," IEEE Trans. Electron. Device Lett. Vol. EDL-2, pp. 95-98, Apr. 1981.
13. Kazmerski, L. L., Polycrystalline and Amorphous Thin Films and Devices, Academic Press, 1980.
14. Private communication with John Andrews, Bell Labs, Murray Hill, NJ.
15. Dumbri, A. C., Masters Thesis entitled High Impedance Loads for MOS Circuits, 1978, Lehigh University.
16. L. Gerzberg, "Monolithic Power-Spectrum Centroid Detector," Ph.D. dissertation, TR No. G557-2, Stanford Univ., Stanford, CA, May 1979.
17. W. R. Knolle and H. R. Maxwell, Jr., "A Model of SIPOS Deposition Based on Infrared Spectroscopic Analysis," J. Electrochem. Society: SOLID STATE SCIENCE AND TECHNOLOGY, October 1980.
18. H. R. Maxwell, Jr. and W. R. Knolle, "Densification of SIPOS," J. Electrochem. Society: SOLID-STATE SCIENCE AND TECHNOLOGY, March 1981.

## XI. BIOGRAPHY

Richard Snyder was born in Scranton, Pennsylvania on December 13, 1948, the son of Richard and Ruth Snyder. He attended Pennsylvania State University from which he graduated in 1968 with an Associate Degree in Electrical and Electronics Technology. Also he graduated with honors from Albright College in 1974 where he received a Bachelor of Science Degree in Physics. Richard has been employed by Bell Laboratories since 1968.